

Towards an understanding of the stability properties of the 3+1 evolution equations in general relativity

Miguel Alcubierre,¹ Gabrielle Allen,¹ Bernd Brügmann,¹ Edward Seidel,^{1,2} and Wai-Mo Suen^{3,4}

¹*Max-Planck-Institut für Gravitationsphysik, Albert-Einstein-Institut, Am Mühlenberg 1, 14476 Golm, Germany*

²*National Center for Supercomputing Applications, Beckman Institute, 405 North Mathews Avenue, Urbana, Illinois 61801*

³*Department of Physics, Washington University, St. Louis, Missouri 63130*

⁴*Physics Department, Chinese University of Hong Kong, Hong Kong*

(Received 31 August 1999; revised manuscript received 8 May 2000; published 21 November 2000)

We study the stability properties of the standard ADM formulation of the 3+1 evolution equations of general relativity through linear perturbations of flat spacetime. We focus attention on modes with zero speed of propagation and conjecture that they are responsible for instabilities encountered in numerical evolutions of the ADM formulation. These zero speed modes are of two kinds: pure gauge modes and constraint violating modes. We show how the decoupling of the gauge by a conformal rescaling can eliminate the problem with the gauge modes. The zero speed constraint violating modes can be dealt with by using the momentum constraints to give them a finite speed of propagation. This analysis sheds some light on the question of why some recent reformulations of the 3+1 evolution equations have better stability properties than the standard ADM formulation.

PACS number(s): 04.25.Dm, 04.30.Db, 95.30.Sf, 97.60.Lf

I. INTRODUCTION

There has been an intense effort in trying to develop numerical relativity for the study of astrophysical phenomena involving black holes and neutron stars. Most investigations in numerical relativity for the last 30 years have been based on the Arnowitt-Deser-Misner (ADM) [1] system of evolution equations and many important results have been obtained in spherical symmetry and axisymmetry. However, in the general three-dimensional (3D) case which is needed for the simulation of realistic astrophysical systems, it has not been possible to obtain long term stable and accurate evolutions (although some good progress has been made, see, e.g., [2–5]). One might argue that present day computational resources are still insufficient to carry out high enough resolution 3D simulations. However, the difficulty is likely to be more fundamental than that. There is no theorem guaranteeing the well-posedness of the initial-boundary value problem for the full ADM system. In particular, one must consider the possibility that free evolutions using the ADM system might be unstable, e.g., against constraint violations in 3D. There are also well-known complications due to the gauge (coordinate) degrees of freedom in the theory. This is one of the major open problems in numerical relativity.

Against this background of the need and failure to obtain long term stable, accurate 3D simulations in numerical relativity, in the last decade there has been a lot of effort looking for alternative formulations of the 3+1 equations, which can be roughly separated in two directions. (I) In the mathematical direction, several first order hyperbolic formulations have been proposed, and conditions on the well posedness of the initial-boundary value problem have been studied [6–23]. Unfortunately there is as yet no evidence that the hyperbolic re-formulations lead to significant improvements in general 3D numerical calculations (despite encouraging results in the spherical symmetric case [11]). (II) In the more “empirical”

direction there have also been various attempts to improve stability and accuracy by modifying the ADM system. To avoid instabilities due to constraint violation, fully or partially constrained evolutions have been tried and the addition of “constraint enforcing terms” into the ADM evolution equations has been proposed and attempted [24,25] (cf. [26]). Methods to better enforce gauge conditions have also been suggested [27]. Most significant and relevant for our present paper is an approach based on separating out the conformal and traceless part of the ADM system, first developed by Shibata and Nakamura [28]. Unfortunately, the strength of the Shibata-Nakamura approach was not widely appreciated, until Baumgarte and Shapiro [29] compared the standard ADM formulation with a modified version of the Shibata-Nakamura formulation on a series of test cases, showing the remarkable stability properties of the conformal-traceless (CT) system. This has triggered much recent research in the community, including what we are reporting here and in a companion paper. There also have been interesting results connecting the conformal approach to the hyperbolic approach [23,30,31].

In this and a companion paper we compare the standard ADM equations to the CT equations of Shibata-Nakamura and Baumgarte-Shapiro in different implementations. In the companion paper [32], we show empirically the strength of this system over the standard ADM equations in numerical evolutions, at least in some of the implementations of the former set of equations. We study in particular the CT formulations in numerical evolutions of strongly gravitating systems (see also [33]) and when coupled to hydrodynamic evolution equations, extending previous studies of weak fields [29] and of predetermined hydrodynamic sources [34]. The main conclusion is that the CT formulation is more stable than the standard ADM formulation in all cases, while it needs more resolution for a given accuracy than ADM in some cases.

In this paper, we aim at developing a mathematical under-

standing of the stability properties of the ADM and the CT equations. Ideally one would like to know if the different systems are well-posed. However, the systems of equations as they stand are mixed first-second order systems and as such are not hyperbolic in any immediate sense. This makes a study of their well-posedness particularly difficult. Because of this fact, we have chosen instead to study linear perturbations of a flat background and do a Fourier analysis. We believe that this analysis, though only valid in the linear regime, reveals important information about the stability properties of the different formulations.

We study in particular two types of zero speed modes that appear in the standard ADM formulation, the ‘‘gauge modes’’ and the ‘‘constraint violating modes,’’ and what they turn into in different implementations of the CT system. The main result of this paper is a conjecture that the zero speed modes are responsible for the instabilities seen in the integration of the ADM system, and a suggestion of how they could be handled to obtain stable evolutions. We stress the point that we do not believe that these instabilities are of numerical origin. Instead, we believe that they correspond to genuine solutions of the exact system of differential equations. A related analysis to the one we present here, but along different lines, was recently carried out by Frittelli and Reula [31].

In Sec. II, we study the linearized ADM equations. In Sec. III we introduce a model problem to help us understand the effect of the zero speed modes. In Sec. IV we discuss the gauge modes, and in Sec. V the constraint violating modes. In Sec. VI, numerical examples are considered. We conclude with Sec. VII. Comments on finite difference approximations to the linearized ADM equations can be found in the Appendix.

A final comment about the language used to describe the solutions to the different systems of equations. We have chosen to refer to all solutions that satisfy the constraints as *physical* solutions, and those that do not as *unphysical*. According to this criterion we will consider pure gauge solutions as physical solutions, even if they contain no real physical information.

II. THE LINEARIZED ADM EQUATIONS

Let us consider first the standard ADM evolution equations for the spatial metric g_{ij} and extrinsic curvature K_{ij} which in vacuum take the form

$$(\partial_t - \mathcal{L}_\beta)g_{ij} = -2\alpha K_{ij}, \quad (1)$$

$$(\partial_t - \mathcal{L}_\beta)K_{ij} = -D_i D_j \alpha + \alpha(R_{ij} + K K_{ij} - 2K_{im} K_j^m), \quad (2)$$

with \mathcal{L}_β the Lie derivative with respect to the shift vector β^i , α the lapse function, D_i the covariant derivative with respect to the spatial metric, R_{ij} the Ricci tensor of the 3-geometry, and $K = g^{ij} K_{ij}$.

Together with the evolution equations, one must also consider the Hamiltonian constraint

$$R + K^2 - K_{ij} K^{ij} = 0, \quad (3)$$

and the momentum constraints

$$D_j(K^{ij} - g^{ij}K) = 0. \quad (4)$$

Let us now take geodesic slicing $\alpha = 1$ and zero shift $\beta^i = 0$, and consider as well a linear perturbation of flat space

$$g_{ij} = \delta_{ij} + h_{ij}, \quad (5)$$

with $h_{ij} \ll 1$. The evolution equations now reduce to

$$\partial_t h_{ij} = -2K_{ij}, \quad (6)$$

$$\partial_t K_{ij} = R_{ij}^{(1)}, \quad (7)$$

where the linearized Ricci tensor is given by

$$R_{ij}^{(1)} = -1/2(\nabla_{\text{flat}}^2 h_{ij} - \partial_i \Gamma_j - \partial_j \Gamma_i) \quad (8)$$

and where we have defined ($h \equiv \text{tr } h_{ij}$)

$$\Gamma_i := \sum_k \partial_k h_{ik} - 1/2 \partial_i h. \quad (9)$$

Notice that Γ_i is just the linearized version of $g^{mn} \Gamma_{mn}^i$.

In the same way, we find that the linearized approximation to the constraints is

$$\sum_k \partial_k f_k = 0 \quad (\text{Hamiltonian}), \quad (10)$$

$$\partial_t f_i = 0 \quad (\text{momentum}) \quad (11)$$

where now

$$f_i := \sum_k \partial_k h_{ik} - \partial_i h. \quad (12)$$

The structure of the constraints is quite interesting. They just state that the vector \vec{f} should be both divergenceless, and time independent. Notice that both these conditions would be trivially satisfied if we were to choose $\vec{f} = 0$, which somewhat counterintuitively amounts to three conditions instead of four. Notice also that asking for a transverse ($\partial_k h_{ik} = 0$) and traceless ($h = 0$) solution means that $\vec{f} = 0$, so the constraints are satisfied automatically. This is precisely what is done when one chooses the standard transverse-traceless (TT) gauge.

Having found the linearized evolution equations, we now proceed to do a Fourier analysis. Without loss of generality (but see Appendix), we can take the plane waves to be moving in the x direction. The result for any other direction can be recovered by a simple tensor rotation later. We then assume that we have a solution of the form

$$h_{ij} = \hat{h}_{ij} e^{i(\omega t - kx)}, \quad (13)$$

$$K_{ij} = \hat{K}_{ij} e^{i(\omega t - kx)}. \quad (14)$$

Equation (6) implies

$$\hat{K}_{ij} = -(i\omega/2)\hat{h}_{ij}. \quad (15)$$

Substituting this into Eq. (7) we find

$$\omega^2 \hat{\mathbf{h}} = k^2 M \hat{\mathbf{h}}, \quad (16)$$

where we have defined the six-dimensional vector

$$\hat{\mathbf{h}} := (\hat{h}_{xx}, \hat{h}_{yy}, \hat{h}_{zz}, \hat{h}_{xy}, \hat{h}_{xz}, \hat{h}_{yz}), \quad (17)$$

and the matrix

$$M = \begin{pmatrix} 0 & 1 & 1 & 0 & 0 & 0 \\ 0 & 1 & 0 & 0 & 0 & 0 \\ 0 & 0 & 1 & 0 & 0 & 0 \\ 0 & 0 & 0 & 0 & 0 & 0 \\ 0 & 0 & 0 & 0 & 0 & 0 \\ 0 & 0 & 0 & 0 & 0 & 1 \end{pmatrix}. \quad (18)$$

One can also find that the constraints (10) and (11) reduce to the three (not four) conditions

$$\hat{h}_{yy} + \hat{h}_{zz} = 0, \quad (19)$$

$$\hat{h}_{xy} = 0, \quad (20)$$

$$\hat{h}_{xz} = 0, \quad (21)$$

where the first one of these equations results from both the Hamiltonian constraint and the x component of the momentum constraint, and the last two result from the y and z components of the momentum constraint, respectively.

It is straightforward to calculate the eigenvalues λ and eigenvectors of the matrix M . They turn out to be as follows.

$\lambda = 0$, with corresponding eigenvectors

$$v_1 = (1, 0, 0, 0, 0, 0), \quad (22)$$

$$v_2 = (0, 0, 0, 1, 0, 0), \quad (23)$$

$$v_3 = (0, 0, 0, 0, 1, 0). \quad (24)$$

$\lambda = 1$, with corresponding eigenvectors

$$v_4 = (2, 1, 1, 0, 0, 0), \quad (25)$$

$$v_5 = (0, 1, -1, 0, 0, 0), \quad (26)$$

$$v_6 = (0, 0, 0, 0, 0, 1). \quad (27)$$

What sort of solutions do the different eigenvectors represent? There are four different types of solutions: two modes that satisfy all the constraints that travel with the speed of light ($\lambda = 1$) represented by the transverse-traceless vectors v_5 and v_6 ; one mode that violates both the Hamiltonian and the x component of the momentum constraints [compare with Eq. (19)], that also travels with the speed of light ($\lambda = 1$) represented by the vector v_4 ; two transverse modes that violate only the momentum constraints [compare

with Eqs. (20) and (21)], and “travel” with speed zero ($\lambda = 0$) represented by the vectors v_2 and v_3 ; one mode that satisfies all the constraints that also has speed zero ($\lambda = 0$) represented by the vector v_1 .

The three constraint satisfying modes are clearly physical solutions. Of these, the two transverse-traceless traveling modes (v_5 and v_6) correspond to the standard gravitational waves. What is the remaining physical mode v_1 ? The only possibility is for it to be a pure gauge mode. To see that this is indeed true all we need to check is that it corresponds to a solution for which the 4-curvature Riemann tensor vanishes. For this we start from the Gauss-Codazzi relations, which to first order are

$${}^{(4)}R_{ijk}^m = {}^{(3)}R_{ijk}^m, \quad (28)$$

$${}^{(4)}R_{ijk}^0 = \partial_k K_{ij} - \partial_j K_{ik}, \quad (29)$$

$${}^{(4)}R_{i0k}^0 = -\partial_t K_{ik}. \quad (30)$$

Now, the fact that v_1 has dependence only on x (by construction), and has a component corresponding only to h_{xx} implies that the right-hand side (RHS) of Eq. (29) vanishes and hence ${}^{(4)}R_{ijk}^0 = 0$. Also, since this mode has zero speed, it corresponds to a mode for which $\partial_t K_{ik} = 0$ which in turn means that ${}^{(4)}R_{i0k}^0 = 0$. Finally, it is not difficult to see that for a solution that depends only on x and for which only h_{xx} is nonzero, the 3-curvature vanishes as well, which tells us that ${}^{(4)}R_{ijk}^m = 0$. The 4-Riemann is then identically zero, so the mode v_1 is a pure gauge mode.

The presence of the zero speed modes (v_1 , v_2 and v_3) is troublesome: They do not represent nonevolving modes as one might think at first sight, but rather they represent modes that annihilate the Ricci tensor. As such, they correspond to solutions for which the extrinsic curvature remains constant in time, and the metric functions grow linearly. With the full nonlinear ADM equations, this linear growth is likely to lead to an instability.

In the next section we use a simple model problem to show how zero speed modes can indeed become unstable in the presence of nonlinear terms.

III. ZERO SPEED MODES: A MODEL PROBLEM

To understand the effects of zero speed modes on stability, we study the simple case of the one-dimensional wave equation with a nonlinear source term F :

$$\partial_t^2 \phi - \epsilon \partial_x^2 \phi = \delta F(\phi, \partial_t \phi, \partial_x \phi). \quad (31)$$

We investigate the stability of the system for different values of ϵ and δ . We will call the system unstable if the magnitude of ϕ grows faster than exponential in time at any fixed value of x , and stable otherwise.

For $\delta = 0$, but ϵ not equal to 0, we have the usual wave equation. A Fourier decomposition of the form used in the last section reveals two eigenmodes with propagation speeds $\lambda = \pm \sqrt{\epsilon}$. The system is stable for all values of ϵ including zero, if there is no source term ($\delta = 0$). With a source term,

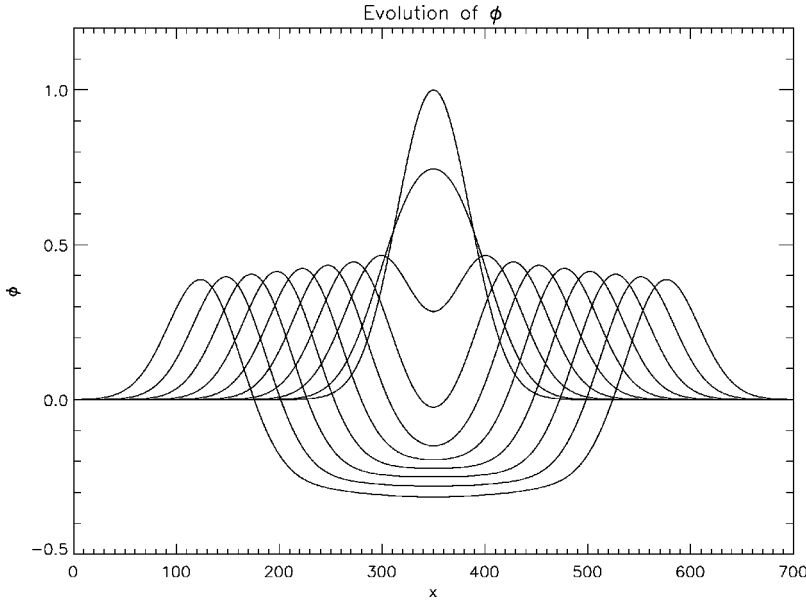


FIG. 1. Evolution of ϕ described by Eq. (33), with $\epsilon=1$ and $\delta=-0.01$ at various times (from $t=0$ to $t=30$ in equal time intervals).

it will still be stable for nonzero ϵ , but *not* so if ϵ becomes zero. For zero ϵ , the two propagation speeds degenerate to zero, and the system is unstable for a general source term. This can be shown analytically by writing Eq. (31) in first order form:

$$\partial_t \begin{pmatrix} \phi \\ D \\ \pi \end{pmatrix} - \begin{pmatrix} 0 & 0 & 0 \\ 0 & 0 & 1 \\ 0 & \epsilon & 0 \end{pmatrix} \partial_x \begin{pmatrix} \phi \\ D \\ \pi \end{pmatrix} = \begin{pmatrix} \pi \\ 0 \\ \delta F \end{pmatrix}, \quad (32)$$

where $D := \partial_x \phi$ and $\pi := \partial_t \phi$. For ϵ not equal to 0, the characteristic matrix (the matrix multiplying the ∂_x term above) has three independent eigenvectors: $(1,0,0)$, $(0,1,\sqrt{\epsilon})$, and $(0,1,-\sqrt{\epsilon})$. The eigenvector matrix and its inverse have bounded norms. The system is therefore strongly hyperbolic, which in turn guarantees its stability [35].

When $\epsilon=0$, two of the eigenvectors become degenerated and the system becomes weakly hyperbolic [35]. For $\delta=0$, the system is still stable, with at most linear growth in ϕ . But for δ nonzero and with a general source term, the system is unstable [35,36].

As an example, we take $F = \phi^2$ in Eq. (33):

$$\partial_t^2 \phi - \epsilon \partial_x^2 \phi = \delta \phi^2. \quad (33)$$

When ϵ is nonzero, there are no zero speed modes and the evolution is stable. In Fig. 1 we show the evolution of ϕ at various times (from $t=0$ to $t=30$ in equal time intervals) for the case of $\epsilon=1$ and $\delta=-0.01$ (the initial data is a Gaussian wave packet). This evolution is very similar to that of a nonlinear gravitational plane wave (see [37]).

Next we tune ϵ down to zero in Eq. (33). The propagation speed of the eigenmodes becomes zero. The initial Gaussian profile now does not propagate, instead it decreases in amplitude initially, becomes negative and eventually blows up. See Fig. 2 for the evolution up to $t=5$, with the same initial data as before. In fact, this system is simple enough to be

solved exactly. One can show that, at given value of x , the solution blows up as $-1/(t-c(x))^2$, where c is a constant depending on the initial value of ϕ at that point. From this it is clear that ϕ in fact becomes infinite after a finite time.

We have studied examples with different source terms and have seen similar behavior, namely the systems become unstable when ϵ goes to zero. To relate more directly this scalar field instability to the ADM equations, we insert variable parameters (ϵ 's) into the linearized ADM system studied in the previous section. We examine the case in which the matrix M [in Eq. (18)] contains variable parameters ϵ_1 , ϵ_2 , and ϵ_3 :

$$M_\epsilon = \begin{pmatrix} \epsilon_1 & 1 & 1 & 0 & 0 & 0 \\ 0 & 1 & 0 & 0 & 0 & 0 \\ 0 & 0 & 1 & 0 & 0 & 0 \\ 0 & 0 & 0 & \epsilon_2 & 0 & 0 \\ 0 & 0 & 0 & 0 & \epsilon_3 & 0 \\ 0 & 0 & 0 & 0 & 0 & 1 \end{pmatrix}. \quad (34)$$

For nonzero (positive) ϵ 's, the corresponding set of second order differential equations has no zero speed modes. To investigate its stability, it is straightforward to break this second order system into a first order system as in the scalar field study above. It is then easy to show that the resulting first order system is strongly hyperbolic and hence stable. As we turn the ϵ 's to zero (recovering the ADM system), zero speed modes appear in the second order system and the corresponding first order system becomes only weakly hyperbolic. This is precisely what happened in the scalar field example above. We hence conjecture that the existence of zero speed modes and the related weak hyperbolicity is at least one of the reasons why the ADM system becomes unstable in numerical evolutions when nonlinear source terms cannot be neglected (i.e., unstable when gravity and/or gauge effects become strong).

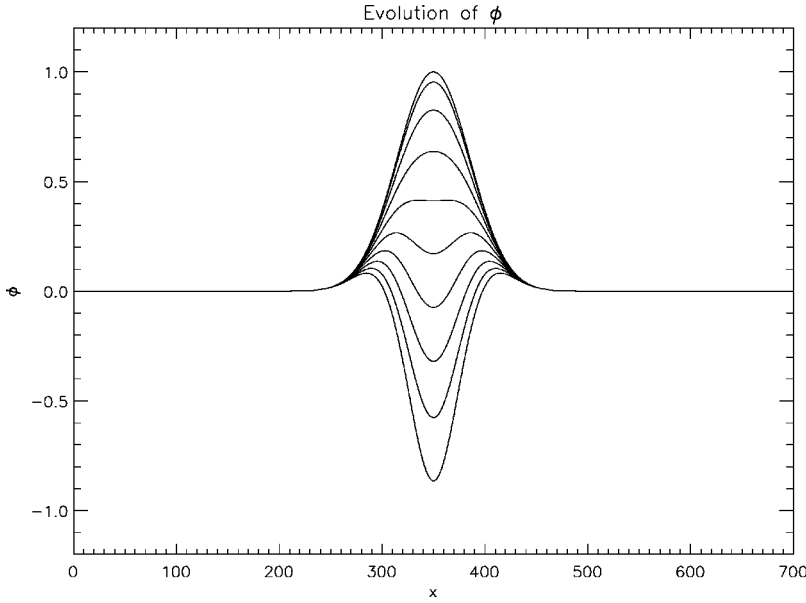


FIG. 2. Evolution of ϕ described by Eq. (31), with $\epsilon=0$ and $\delta=-0.01$ at various times (from $t=0$ to $t=30$ in equal time intervals).

As an explicit example of such a transition between linear growth and nonlinear blow up in the ADM case, we note the well known case of focusing in geodesic slicing. It is precisely the zero speed gauge mode discussed in the previous section the one that represents the focusing of geodesic slicing. In the full nonlinear case this focusing produces a coordinate singularity causing a blow up in a finite time.

One last comment comparing different blowing up solutions is in order. We note that the nonlinear wave equation (33) described above has solutions that blow up in a finite time even in the case of a nonzero wave speed. For $\epsilon=1$ and $\delta=1$, two such solutions are $\phi = -6/(t-c)^2$ (with c a spatial constant) and $\phi = -4/(t^2-x^2)$. However, these “blowing up solutions” are fundamentally different from those in the zero-wave-speed case we focused on above. These “blowing up solutions” are blowing up in a global manner, and can come into existence in our numerical evolutions only if we choose boundary conditions that allow them. In numerical evolutions (at least those considered in this paper) we typically start the evolution at a certain initial time in a compact computational domain with a certain chosen set of boundary conditions. The “blowing up solutions,” which are blowing up in a global manner can be excluded by an appropriate set of boundary conditions. On the other hand, in the case when $\epsilon=0$ and $\delta>0$, the unstable solution involves an arbitrary function of x . One can see that any initial data with positive ϕ will cause a local blow up, independently of its initial profile. It cannot be excluded by choosing boundary conditions. The locality of the instability is the crux of the problem making it dangerous in numerical evolutions.

In the next sections, we focus on the zero speed modes in the case of the Einstein equations. We show how one can deal separately with the gauge mode and the constraint violating modes.

IV. DEALING WITH THE GAUGE MODE: DECOUPLING K

In trying to deal with the zero speed modes, we will first concentrate on the pure gauge mode: the mode v_1 , associated

with h_{xx} in the analysis of Sec. II. Since this mode satisfies all the constraints, it represents a physical solution of the evolution equations (even if it only corresponds to a non-trivial evolution of the coordinate system), and hence cannot be eliminated. The most we can hope to achieve is to decouple it from the rest of the evolution equations, so that it will be immune to possible numerical errors, in particular those coming from the complicated Ricci tensor terms driving the evolution.

Remarkably, such a decoupling is not difficult to achieve. Following [29,28,30] we first conformally rescale the metric in the following way:

$$\tilde{g}_{ij} = e^{-4\phi} g_{ij}, \quad (35)$$

with ϕ chosen in such a way that the rescaled metric \tilde{g}_{ij} has unit determinant,

$$\phi = \frac{1}{12} \log g. \quad (36)$$

We also define the conformally rescaled, trace-free part of the extrinsic curvature K_{ij} as

$$\tilde{A}_{ij} = e^{-4\phi} \left(K_{ij} - \frac{1}{3} g_{ij} K \right). \quad (37)$$

The ADM equations (1) and (2) can now be rewritten as the following system of 14 evolution equations:

$$(\partial_t - \mathcal{L}_\beta) \phi = -\frac{\alpha}{6} K, \quad (38)$$

$$(\partial_t - \mathcal{L}_\beta) \tilde{g}_{ij} = -2\alpha \tilde{A}_{ij}, \quad (39)$$

$$(\partial_t - \mathcal{L}_\beta) K = -D^i D_i \alpha + \alpha (R + K^2), \quad (40)$$

$$(\partial_t - \mathcal{L}_\beta) \tilde{A}_{ij} = e^{-4\phi} (-D_i D_j \alpha + \alpha R_{ij})^{TF} \quad (41)$$

$$+ \alpha(K\tilde{A}_{ij} - 2\tilde{A}_{il}\tilde{A}_j^l), \quad (42)$$

subject to the extra constraints $\tilde{g} = 1$, $\text{tr}\tilde{A} = 0$.

The Hamiltonian and momentum constraints now become as

$$R - \tilde{A}_{ij}\tilde{A}^{ij} + 2K^2/3 = 0, \quad (43)$$

$$\tilde{D}_j(\tilde{A}^{ij} - 2\tilde{g}^{ij}K/3) + 6\tilde{A}^{ij}\partial_j\phi = 0. \quad (44)$$

Notice that now we have separated out the ‘‘gauge’’ variables $\{\phi, K\}$, but we have not yet decoupled the evolution equation for K from the Ricci tensor. This last step can be achieved by making use of the Hamiltonian constraint above. Doing this, we can eliminate all reference to the Ricci tensor from the evolution equation for K . One can also use the Hamiltonian constraint to eliminate the Ricci scalar from the evolution equation for \tilde{A}_{ij} . In fact, one can consider adding an arbitrary multiple of the Hamiltonian constraint to this equation. We will then consider the evolution equations

$$(\partial_t - \mathcal{L}_\beta)\phi = -\frac{\alpha}{6}K, \quad (45)$$

$$(\partial_t - \mathcal{L}_\beta)\tilde{g}_{ij} = -2\alpha\tilde{A}_{ij}, \quad (46)$$

$$(\partial_t - \mathcal{L}_\beta)K = -D^i D_i \alpha + \alpha\left(\tilde{A}_{ij}\tilde{A}^{ij} + \frac{1}{3}K^2\right), \quad (47)$$

$$\begin{aligned} (\partial_t - \mathcal{L}_\beta)\tilde{A}_{ij} &= e^{-4\phi}(-D_i D_j \alpha + \alpha R_{ij})^{TF} \\ &+ \frac{\alpha}{3}\sigma\tilde{g}_{ij}\left(R - \tilde{A}_{ij}\tilde{A}^{ij} + \frac{2}{3}K^2\right) \\ &+ \alpha(K\tilde{A}_{ij} - 2\tilde{A}_{il}\tilde{A}_j^l). \end{aligned} \quad (48)$$

Notice that $\sigma = 1$ will correspond to the case when the Ricci scalar is eliminated from the evolution equation for \tilde{A}_{ij} .

As before, we will now concentrate on the case of geodesic slicing $\alpha = 1$ with zero shift $\beta^i = 0$, and consider a linear perturbation of flat space,

$$\tilde{g}_{ij} = \delta_{ij} + \tilde{h}_{ij}. \quad (49)$$

The evolution equations then become

$$\partial_t \phi = -K/6, \quad (50)$$

$$\partial_t \tilde{h}_{ij} = -2\tilde{A}_{ij}, \quad (51)$$

$$\partial_t K = 0, \quad (52)$$

$$\partial_t \tilde{A}_{ij} = R_{ij}^{(1)} - \delta_{ij}R^{(1)}(1 - \sigma)/3, \quad (53)$$

with $R_{ij}^{(1)}$ the linear Ricci tensor. Notice now that to linear order K does not evolve at all: to linear order the evolution of the gauge variables $\{\phi, K\}$ is therefore completely trivial. In particular, if K is chosen to be zero initially, it will remain exactly zero: no need for any exact cancellation.

Now, quite generally the Ricci tensor can be separated into

$$R_{ij} = \tilde{R}_{ij} + R_{ij}^\phi. \quad (54)$$

The first term above \tilde{R}_{ij} is the Ricci tensor associated with the conformal metric which to linear order is

$$\tilde{R}_{ij}^{(1)} = -1/2(\nabla_{\text{flat}}^2 \tilde{h}_{ij} - \partial_i \tilde{\Gamma}_j - \partial_j \tilde{\Gamma}_i), \quad (55)$$

with the $\tilde{\Gamma}_i$ defined just as before, but now using the conformal metric

$$\tilde{\Gamma}_i := \sum_k \partial_k \tilde{h}_{ik} - 1/2 \partial_i \tilde{h}. \quad (56)$$

The second term in Eq. (54) is the part of the Ricci tensor coming from the conformal factor ϕ which to first order is

$$R_{ij}^{\phi(1)} = -2(\partial_i \partial_j \phi + \delta_{ij} \nabla_{\text{flat}}^2 \phi). \quad (57)$$

Notice that one can easily prove that

$$\det \tilde{g}_{ij} = 1 \Rightarrow \tilde{h} = 0, \quad (58)$$

so we could in principle eliminate the second term in Eq. (56). As we will see below, this is a bad idea, so here we will just add instead a parameter ξ that will be equal to 0 if we eliminate \tilde{h} , and equal to 1 if we do not (but see the next section, where the $\tilde{\Gamma}$'s are promoted to independent variables). We can then rewrite the first order Ricci tensor as

$$\begin{aligned} R_{ij}^{(1)} &= -1/2[\nabla_{\text{flat}}^2 \tilde{h}_{ij} + \xi \partial_i \partial_j \tilde{h}] + \sum_k \partial_k \partial_{(i} \tilde{h}_{j)k} \\ &- 2[\partial_i \partial_j \phi + \delta_{ij} \nabla_{\text{flat}}^2 \phi]. \end{aligned} \quad (59)$$

Using this we can find the linearized version of the constraints

$$\sum_i \partial_i \tilde{f}_i = 0 \quad (\text{Hamiltonian}), \quad (60)$$

$$\partial_t \tilde{f}_i = 0 \quad (\text{momentum}), \quad (61)$$

where now

$$\tilde{f}_i := \sum_j \partial_j \tilde{h}_{ij} - 8 \partial_i \phi. \quad (62)$$

As before, having found the linearized form of the evolution equations, we will proceed to make a Fourier analysis of the system. We then assume that we have a solution of the form

$$\phi = \hat{\phi} e^{i(\omega t - kx)}, \quad (63)$$

$$\tilde{h}_{ij} = \hat{h}_{ij} e^{i(\omega t - kx)}, \quad (64)$$

$$K = \hat{K} e^{i(\omega t - kx)}, \quad (65)$$

$$\tilde{A}_{ij} = \hat{A}_{ij} e^{i(\omega t - kx)}. \quad (66)$$

The evolution equations for ϕ and \tilde{h}_{ij} imply

$$\hat{K} = -6i\omega \hat{\phi}, \quad \hat{A}_{ij} = -\frac{i}{2} \omega \hat{h}_{ij}. \quad (67)$$

Substituting this into the evolution equations for K and \tilde{A}_{ij} we find

$$\omega^2 \hat{\mathbf{h}} = k^2 M \hat{\mathbf{h}}, \quad (68)$$

where now \mathbf{h} is a seven-dimensional vector

$$\hat{\mathbf{h}} := (\hat{\phi}, \hat{h}_{xx}, \hat{h}_{yy}, \hat{h}_{zz}, \hat{h}_{xy}, \hat{h}_{xz}, \hat{h}_{yz}), \quad (69)$$

and

$$M = \begin{pmatrix} 0 & 0 & 0 & 0 & 0 & 0 & 0 \\ m_{21} & m_{22} & m_{23} & m_{24} & 0 & 0 & 0 \\ m_{31} & m_{32} & m_{33} & m_{34} & 0 & 0 & 0 \\ m_{41} & m_{42} & m_{43} & m_{44} & 0 & 0 & 0 \\ 0 & 0 & 0 & 0 & 0 & 0 & 0 \\ 0 & 0 & 0 & 0 & 0 & 0 & 0 \\ 0 & 0 & 0 & 0 & 0 & 0 & 1 \end{pmatrix}, \quad (70)$$

with

$$m_{21} = 8 - 16(1 - \sigma)/3, \quad (71)$$

$$m_{22} = (\xi - 1)(1 - (1 - \sigma)/3), \quad (72)$$

$$m_{23} = m_{24} = \xi - (\xi + 1)(1 - \sigma)/3, \quad (73)$$

$$m_{31} = m_{41} = 4 - 16(1 - \sigma)/3, \quad (74)$$

$$m_{32} = m_{42} = -(\xi - 1)(1 - \sigma)/3, \quad (75)$$

$$m_{33} = m_{44} = 1 - (\xi + 1)(1 - \sigma)/3, \quad (76)$$

$$m_{34} = m_{43} = -(\xi + 1)(1 - \sigma)/3. \quad (77)$$

The Hamiltonian and momentum constraints now reduce to the three equations (again, not four)

$$\hat{h}_{xx} - 8 \hat{\phi} = 0, \quad (78)$$

$$\hat{h}_{xy} = 0, \quad (79)$$

$$\hat{h}_{xz} = 0, \quad (80)$$

where as before, the first condition results from both the Hamiltonian constraint and the x component of the momentum constraints.

The eigenvalues λ and eigenvectors of the matrix (70) are now somewhat more complicated. Let us consider first the eigenvalues on their own. They are $\lambda = 0$, with multiplicity 3, $\lambda = 1$, with multiplicity 2, and $\lambda = (\sigma - 1 + 3\xi\sigma \pm \eta)/6$, with

$$\eta = [1 + \sigma(34 - 42\xi) + \sigma^2(1 + 3\xi)^2]^{1/2}. \quad (81)$$

There are a couple of things to notice from the last two eigenvalues. First, notice that if we take $\sigma = 0$, one of these eigenvalues is always negative, which implies the existence of an exponentially growing mode, i.e., we have an unstable system of equations. So we *must* add some multiple of the Hamiltonian constraint to the evolution equation of \tilde{A}_{ij} . How much we need to add will depend on the value of ξ . Moreover, with a little algebra one can also see that taking $\xi = 0$ results as well in a negative eigenvalue. This means that if we had decided to use the constraint $\tilde{h} = 0$ ($\xi = 0$) in the expression for the Ricci tensor, we would again have an unstable system of evolution equations. A safe value for ξ turns out to be $\xi = 1$. If we choose this, the characteristic structure of the matrix (70) becomes the following.

$\lambda = 0$, with corresponding eigenvectors

$$v_1 = (1, 8, -4, -4, 0, 0, 0), \quad (82)$$

$$v_2 = (0, 0, 0, 0, 1, 0, 0), \quad (83)$$

$$v_3 = (0, 0, 0, 0, 0, 1, 0), \quad (84)$$

$$v_4 = (0, 1, 0, 0, 0, 0, 0). \quad (85)$$

$\lambda = 1$, with eigenvectors

$$v_5 = (0, 0, 1, -1, 0, 0, 0), \quad (86)$$

$$v_6 = (0, 0, 0, 0, 0, 0, 1). \quad (87)$$

$\lambda = (4\sigma - 1)/3$, with eigenvector

$$v_7 = (0, (4\sigma + 2), (4\sigma - 1), (4\sigma - 1), 0, 0, 0). \quad (88)$$

Notice the last eigenvalue $\lambda = (4\sigma - 1)/3$ will only be positive for $\sigma \geq 1/4$, which tells us that we must add at least this much of the Hamiltonian constraint to the evolution equation for \tilde{A}_{ij} . A natural choice is to take $\sigma = 1$. This

corresponds to completely eliminating the Ricci scalar from this equation, and results in the eigenvalue reducing to the physical speed of light.

The type of solutions that the different eigenvectors represent are (1) Two physical solutions that travel with the speed of light ($\lambda = 1$) represented by the transverse-traceless vectors v_5 and v_6 , (2) one mode that violates the Hamiltonian constraint, the x component of the momentum constraint, and the constraint $\tilde{h}=0$, that travels with the speed equal to the square root of $(4\sigma-1)/3$, represented by the vector v_7 , (3) two modes that violate only the momentum constraints, and “travel” with speed zero ($\lambda=0$) represented by the vectors v_2 and v_3 , (4) one mode that violates the Hamiltonian constraint, the x component of the momentum constraint, and the constraint $\tilde{h}=0$ that has speed zero ($\lambda=0$) represented by the vector v_4 , and (5) one pure gauge mode (satisfying all the constraints) that travels with speed zero ($\lambda=0$) represented by the vector v_1 .

The structure of these eigenvalues and eigenvectors tells us in the first place that one has to be careful in the way in which different constraints are added to the evolution equations. The simple statement that one is in principle free to add multiples of constraints to evolution equations is true only if one does not worry about the stability of the final system. In this case we have seen how using blindly the constraint $\tilde{h}=0$ to simplify one of the equations results in the appearance of an unstable mode, and how neglecting to use the Hamiltonian constraint in another equation also gives rise to an unstable mode. A similar point has also been made in [38] in the context of adding multiples of the Hamiltonian constraint to the standard ADM evolution equations.

From the characteristic structure described above, we can see that we now have four zero speed modes instead of three (assuming we do take $\xi=1$), so the situation would seem worse than before. Three of these modes are constraint violating, and we will worry about them in the next section. What about the gauge mode? The gauge mode is of course still there, and it still has zero speed (as it should), but now it is in a much more convenient form. From looking at v_1 we see that its evolution depends on the evolution equation for ϕ , which we have seen is trivial in the linear and nonlinear case, and the evolution of the traceless part of \tilde{h}_{ij} , which is also trivial as long as the constraint $\text{tr}\tilde{A}=0$ is satisfied [see Eq. (51)]. The important point is the following: the fact that this mode evolves trivially is now the consequence of the simple *algebraic* constraint $\text{tr}\tilde{A}=0$, and is independent of exact cancellations in *derivatives* of the metric that appear in the Ricci tensor. This provides an easy way to control the mode: Numerically setting $\text{tr}\tilde{A}$ to zero after each step of the evolution ensures that the gauge mode cannot grow.

A comment is in order here. It has been recognized for some time [10,11,18] that gauge modes can propagate with arbitrary speeds. The analysis presented above shows that constraint violating modes can do the same. Often one does not think about these modes because they are unphysical, and one can avoid exciting them with an appropriate choice of initial data. However, from a numerical point of view,

they will never really vanish and as we have just seen they can have important consequences on the stability of our evolutions. Even when these modes have a real speed of propagation (as opposed to an imaginary speed indicating an instability on the analytic level), if that speed is larger than the speed of light they can cause numerical instabilities if one forgets about their existence and chooses a time step based only on the extension of the physical light cones.

V. DEALING WITH THE CONSTRAINT VIOLATING MODES: USING THE MOMENTUM CONSTRAINTS

In the previous section we have seen how separating out the gauge variables $\{\phi, K\}$ provides a way to control the zero speed gauge mode. This still leaves us with the zero speed constraint violating modes to worry about. Here we will show how those modes can be dealt with by using the momentum constraints to modify the evolution equations of extra first order degrees of freedom.

The idea of using the momentum constraints to modify the evolution equations is at the core of many recent hyperbolic reformulations of the Einstein equations [10–13]. In particular, the use of the momentum constraints to obtain evolution equations for extra first order variables can be traced back to the Bona-Massó formulation [10,11]. Here we will follow for simplicity the approach of Baumgarte and Shapiro [29] (a very similar approach has been used before by Shibata and Nakamura [28]).

We will again concentrate on the case of geodesic slicing $\alpha=1$ with zero shift $\beta^i=0$, and consider a linear perturbation of flat space. The linearized evolution equations were given by Eqs. (50)–(53). The Ricci tensor that appears in the evolution equation for \tilde{A}_{ij} was separated as

$$R_{ij}^{(1)} = \tilde{R}_{ij}^{(1)} + R_{ij}^{\phi(1)}, \quad (89)$$

with

$$\tilde{R}_{ij}^{(1)} = -1/2(\nabla_{\text{flat}}^2 \tilde{h}_{ij} - \partial_i \tilde{\Gamma}_j - \partial_j \tilde{\Gamma}_i) \quad (90)$$

and

$$R_{ij}^{\phi(1)} = -2(\partial_i \partial_j \phi + \delta_{ij} \nabla_{\text{flat}}^2 \phi). \quad (91)$$

Now, instead of writing the quantities $\tilde{\Gamma}_i$ in terms of their definition (56) as we did before, we will promote them to independent quantities, and use Eq. (56) only to obtain their initial values. We will then need an evolution equation for the $\tilde{\Gamma}_i$. This we can obtain trivially from Eqs. (56) and (51):

$$\partial_t \tilde{\Gamma}_i = -2 \sum_k \partial_k \tilde{A}_{ki} + \partial_i \text{tr} \tilde{A}. \quad (92)$$

Notice that we can use the fact that \tilde{A}_{ij} is supposed to be traceless to eliminate the last term above. However, we still do not know if this will turn out to be a good idea or not, so instead we again introduce a parameter ξ and write

$$\partial_t \tilde{\Gamma}_i = -2 \sum_k \partial_k \tilde{A}_{ki} + \xi \partial_i \text{tr } \tilde{A}. \quad (93)$$

There is still one extra modification we want to make to this evolution equation: We will add to it a multiple of the momentum constraints (61) to obtain

$$\partial_t \tilde{\Gamma}_i = 2(m-1) \sum_k \partial_k \tilde{A}_{ki} + \xi \partial_i \text{tr } \tilde{A} - \frac{4m}{3} \partial_i K, \quad (94)$$

with m arbitrary. Equation (94) above is our final evolution equation for the $\tilde{\Gamma}_i$. Keeping the $\tilde{\Gamma}_i$ as independent variables, we also have to remember that we have introduced the extra constraints $\tilde{\Gamma}_i = \sum_k \partial_k \tilde{h}_{ik}$.

For the Fourier analysis, we again consider plane waves moving along the x direction. From the evolution equations for ϕ and \tilde{h}_{ij} we find

$$\hat{K} = -6i\omega\hat{\phi}, \quad \hat{A}_{ij} = -\frac{i}{2}\omega\hat{h}_{ij}, \quad (95)$$

Substituting this in the evolution equations for $\tilde{\Gamma}_i$ we obtain

$$\hat{\Gamma}_x = -ik[(m-1 + \xi/2)\hat{h}_{xx} + \xi/2(\hat{h}_{yy} + \hat{h}_{zz}) - 8m\hat{\phi}], \quad (96)$$

$$\hat{\Gamma}_y = -ik(m-1)\hat{h}_{xy}, \quad (97)$$

$$\hat{\Gamma}_z = -ik(m-1)\hat{h}_{xz}. \quad (98)$$

And finally, substituting all these results back into the evolution equations for K and \tilde{A}_{ij} we find

$$\omega^2 \hat{\mathbf{h}} = k^2 M \hat{\mathbf{h}}, \quad (99)$$

where \mathbf{h} is the same as before

$$\hat{\mathbf{h}} := (\hat{\phi}, \hat{h}_{xx}, \hat{h}_{yy}, \hat{h}_{zz}, \hat{h}_{xy}, \hat{h}_{xz}, \hat{h}_{yz}), \quad (100)$$

and where the matrix M is now

$$M = \begin{pmatrix} 0 & 0 & 0 & 0 & 0 & 0 & 0 \\ m_{21} & m_{22} & m_{23} & m_{24} & 0 & 0 & 0 \\ m_{31} & m_{32} & m_{33} & m_{34} & 0 & 0 & 0 \\ m_{41} & m_{42} & m_{43} & m_{44} & 0 & 0 & 0 \\ 0 & 0 & 0 & 0 & m & 0 & 0 \\ 0 & 0 & 0 & 0 & 0 & m & 0 \\ 0 & 0 & 0 & 0 & 0 & 0 & 1 \end{pmatrix}, \quad (101)$$

with

$$m_{21} = 8(1-2m) - 16(1-m)(1-\sigma)/3, \quad (102)$$

$$m_{22} = (2m + \xi - 1)(1 - (1-\sigma)/3), \quad (103)$$

$$m_{23} = m_{24} = \xi - (\xi + 1)(1-\sigma)/3, \quad (104)$$

$$m_{31} = m_{41} = 4 - 16(1-m)(1-\sigma)/3, \quad (105)$$

$$m_{32} = m_{42} = -(2m + \xi - 1)(1-\sigma)/3, \quad (106)$$

$$m_{33} = m_{44} = 1 - (\xi + 1)(1-\sigma)/3, \quad (107)$$

$$m_{34} = m_{43} = -(\xi + 1)(1-\sigma)/3. \quad (108)$$

Notice that introducing the $\tilde{\Gamma}_i$ as independent variables by itself does not change our analysis based on M , which is obtained by eliminating the $\hat{\Gamma}_i$. But the evolution equations for the $\tilde{\Gamma}_i$ motivate the introduction of the parameter m , whose effect we consider now. The eigenvalues of the matrix (101) turn out to be $\lambda=0$, with multiplicity 1, $\lambda=m$, with multiplicity 2, $\lambda=1$, with multiplicity 2, and $\lambda=(1/6)[b \pm (b^2 - c)^{1/2}]$, with

$$b = -1 + \sigma + 3\xi\sigma + 2m(2 + \sigma), \quad (109)$$

$$c = 36\sigma(-1 + \xi + 2m). \quad (110)$$

The last two eigenvalues are quite complicated, so we will concentrate for the moment on the particular case $\sigma=1$. In that case the eigenvalues and eigenvectors of M reduce to the following.

$\lambda=0$, with corresponding eigenvector

$$v_1 = (1, 8, -4, -4, 0, 0, 0). \quad (111)$$

$\lambda=m$, with corresponding eigenvectors

$$v_2 = (0, 0, 0, 0, 1, 0, 0), \quad (112)$$

$$v_3 = (0, 0, 0, 0, 0, 1, 0). \quad (113)$$

$\lambda=1$, with eigenvectors

$$v_4 = (0, 2\xi/(2-2m-\xi), 1, 1, 0, 0, 0), \quad (114)$$

$$v_5 = (0, 0, 1, -1, 0, 0, 0), \quad (115)$$

$$v_6 = (0, 0, 0, 0, 0, 0, 1). \quad (116)$$

$\lambda=2m + \xi - 1$, with eigenvector

$$v_7 = (0, 1, 0, 0, 0, 0, 0). \quad (117)$$

And the type of solutions represented are (1) two physical solutions that travel with the speed of light ($\lambda=1$) represented by the transverse-traceless vectors v_5 and v_6 , (2) one mode that violates the Hamiltonian constraint, the x component of the momentum constraints, and the constraint $\tilde{h}=0$ that also travels with the speed of light ($\lambda=1$) represented by the vector v_4 , (3) two modes that violate only the momentum constraints, and travel with speed $m^{1/2}$ represented by the vectors v_2 and v_3 , (4) one mode that violates the Hamiltonian constraint, the x component of the momentum constraints and the constraint $\tilde{h}=0$ that has speed $(2m + \xi - 1)^{1/2}$ represented by the vector v_7 , and (5) one pure gauge mode (satisfying all the constraints) that travels with speed zero ($\lambda=0$) represented by the vector v_1 .

Notice first that all constraint violating modes have now acquired a nonzero speed. If we want to have all eigenvalues non-negative (and hence all speeds real), we must have

$$m \geq 0, \quad (118)$$

and

$$2m + \xi - 1 \geq 0 \Rightarrow m \geq \frac{1 - \xi}{2}. \quad (119)$$

In particular, if we take $\xi = 0$ (that is if we use the fact that $\text{tr} \tilde{A} = 0$ in the evolution equation for $\tilde{\Gamma}_i$) then we must have $m > 1/2$. So in order to have a stable system we *must* add a finite multiple of the momentum constraints to the evolution equation for $\tilde{\Gamma}_i$. If we fail to use the momentum constraints, the system will have an exponentially growing mode. This is consistent with the results of the last section, where we did not have the Γ_i (which in some sense is equivalent to not using the momentum constraints), and we found that taking $\xi = 0$ resulted in an unstable system.

Notice also that if we take

$$m = 1, \quad \xi = 0, \quad (120)$$

then we have one zero speed mode and six modes that travel with the speed of light. This is precisely the choice made by Baumgarte and Shapiro in [29], so the result above explains why it was necessary in their case to add a multiple of the momentum constraints, and also why one should expect to have only the speed of light as a characteristic speed in their system. In the case $m = 1$, $\xi = 0$, the eigenvector v_4 might appear at first sight to be singular, but from the form that the matrix M takes in this particular case it is not difficult to show that in fact v_4 is replaced by $(0, 0, 1, 1, 0, 0, 0)$ with all other eigenvectors remaining unchanged. The only zero speed mode left is the pure gauge mode v_1 , but as we have seen before, its evolution does not rely any more on exact cancellations in the Ricci tensor.

Finally, let us consider again the case when $\sigma \neq 1$, but now keeping $m = 1$ and $\xi = 0$. In this case the eigenvalues and eigenvectors become the following.

$\lambda = 0$, with corresponding eigenvector

$$v_1 = (1, 8, -4, -4, 0, 0, 0). \quad (121)$$

$\lambda = 1$, with corresponding eigenvectors

$$v_2 = (0, 0, 0, 0, 1, 0, 0), \quad (122)$$

$$v_3 = (0, 0, 0, 0, 0, 1, 0), \quad (123)$$

$$v_4 = (0, -2, 1, 1, 0, 0, 0), \quad (124)$$

$$v_5 = (0, 0, 1, -1, 0, 0, 0), \quad (125)$$

$$v_6 = (0, 0, 0, 0, 0, 0, 1). \quad (126)$$

$\lambda = \sigma$, with eigenvector

$$v_7 = (0, 1, 1, 1, 0, 0, 0). \quad (127)$$

We see now that depending on how large a multiple of the Hamiltonian constraint we add to the evolution equation of \tilde{A}_{ij} , we can change the speed of propagation of the mode that represents the trace of \tilde{h}_{ij} (and hence the trace of \tilde{A}_{ij}). If we do not use the Hamiltonian constraint at all ($\sigma = 0$), we will again have a zero speed unphysical mode. However, this is not as bad as it might seem because in practice this mode is very easy to control since it will vanish if one imposes the algebraic constraint $\text{tr} \tilde{A} = 0$.

VI. NUMERICAL EXAMPLES: STABILITY OF MINKOWSKI SPACETIME

To compare the stability properties of the different systems in a simple situation we will consider the evolution of Minkowski spacetime, with a flat initial slice, but with a nontrivial spatial coordinate system. Since the extrinsic curvature is zero, the spacetime should then remain static. Numerically, of course, the Ricci tensor will not be exactly zero, so we can expect some nontrivial evolution, but if the system is stable we will only have spurious numerical noise that should propagate away. If the system is unstable, however, we can expect that the numerical noise will slowly grow in amplitude. We will be evolving the full nonlinear equations, so the initially slow growth of the numerical noise can be expected to trigger nonlinear growth at late times.

In order to obtain our initial metric, we start from the flat space metric in spherical coordinates

$$dl^2 = dr^2 + r^2 d\Omega^2, \quad (128)$$

with $d\Omega^2$ the solid angle element. We then make the following coordinate transformation:

$$r = \tilde{r}(1 - af(\tilde{r})), \quad (129)$$

with $0 \leq a < 1$ and $f(\tilde{r})$ a smooth monotonously decreasing function that is 1 for small \tilde{r} and 0 for large \tilde{r} . The particular form of the function f that we will use here is a Gaussian

$$f(\tilde{r}) = e^{-\tilde{r}^2/\sigma^2}. \quad (130)$$

In terms of the new radial coordinate the metric becomes

$$dl^2 = g_{11} d\tilde{r}^2 + \tilde{r}^2 g_{22} d\Omega^2, \quad (131)$$

with

$$g_{11} = [1 - a(f + \tilde{r}f')]^2, \quad (132)$$

$$g_{22} = (1 - af)^2. \quad (133)$$

Finally, for our 3D evolutions we transform this metric to Cartesian coordinates in the standard way,

$$x = \tilde{r} \sin \theta \cos \phi, \quad (134)$$

$$y = \tilde{r} \sin \theta \sin \phi, \quad (135)$$

$$z = \tilde{r} \cos \theta. \quad (136)$$

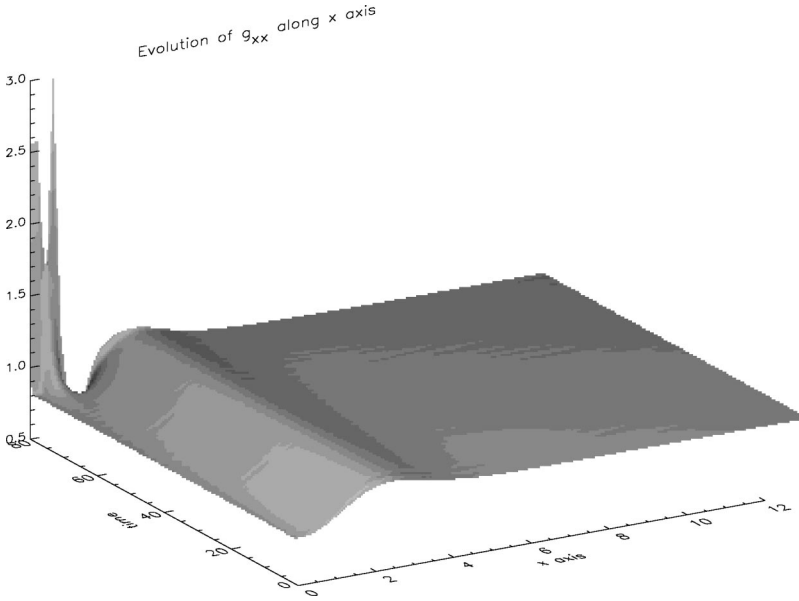


FIG. 3. Surface plot of g_{xx} along the x axis as a function of time for the simulation using the standard ADM formulation.

So our initial metric is

$$g_{xx} = [x^2 g_{11} + (y^2 + z^2) g_{22}] / \tilde{r}^2, \quad (137)$$

$$g_{yy} = [y^2 g_{11} + (x^2 + z^2) g_{22}] / \tilde{r}^2, \quad (138)$$

$$g_{zz} = [z^2 g_{11} + (x^2 + y^2) g_{22}] / \tilde{r}^2, \quad (139)$$

$$g_{xy} = xy(g_{11} - g_{22}) / \tilde{r}^2, \quad (140)$$

$$g_{xz} = xz(g_{11} - g_{22}) / \tilde{r}^2, \quad (141)$$

$$g_{yz} = yz(g_{11} - g_{22}) / \tilde{r}^2. \quad (142)$$

We must also say something about the gauge conditions used. For simplicity, we will use a zero shift vector. For the lapse we could try geodesic slicing, but even small numerical

perturbations will cause focusing (we are evolving the full nonlinear Einstein equations). It is better to use a slicing that can react to the evolution and can propagate away spurious numerical waves. Harmonic slicing is ideal for our purposes. It is defined via the following evolution equation for the lapse:

$$\partial_t \alpha = -\alpha^2 K. \quad (143)$$

Since K is initially set to 0, the lapse should remain 1 if the evolution is exact.

Finally, a comment about boundary conditions. We have used a very simple “zero order extrapolation” boundary condition, that is, we update the boundary by just copying the value of a given field from its value one grid point in (along the normal direction to the boundary). This condition is not very physical, nor does it allow waves to leave the computational grid cleanly enough, but it is very robust, and can be used with all the different formulations studied here in a stable way (at least for the time scales under study). Since our emphasis is on the stability of the interior evolu-

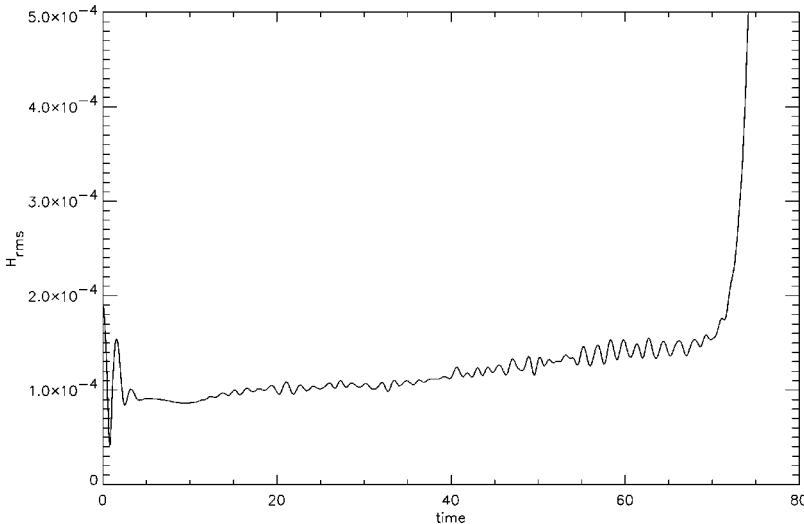


FIG. 4. Root mean square of the Hamiltonian constraint as a function of time for the simulation using the standard ADM formulation.

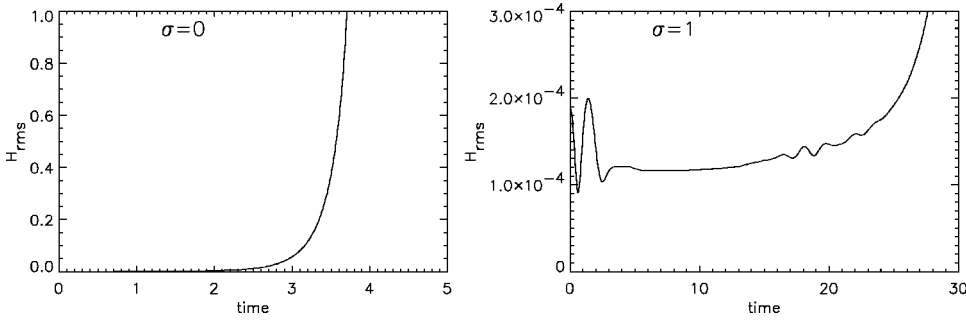


FIG. 5. Root mean square of the Hamiltonian constraint as a function of time for the simulation using the standard CT formulation with $\xi=0$ and two different values of σ .

tion, we are content with having a stable boundary condition. We have used more sophisticated boundary conditions in various cases, but it is difficult to find one that will remain stable for all the evolution systems considered.

We now present results of simulations performed with the different systems. The numerical method used in all these simulations was the so-called ‘‘iterative Crank-Nicholson’’ (ICN) scheme with three iterations. We have found that three iterations are enough to obtain a stable, second order accurate numerical scheme [32].

First we show the results of a simulation using the standard ADM formulation for the case when $a=0.1$ and $\sigma=2$. For this simulation we used a grid with 64^3 points and a resolution on $\Delta x=0.2$. Figure 3 shows a surface plot of g_{xx} along the x axis as a function of time. We see that g_{xx} keeps its initial shape for some time, but at late times it starts to fall apart near the center. The simulation finally crashes at $t=79$. Figure 4 shows the root mean square (rms) of the Hamiltonian constraint over the numerical grid as a function of time. We see that for a long time there is an essentially linear growth of the rms of the Hamiltonian constraint superimposed with small oscillations, just what we expect from the linear analysis of the previous sections. At late times, however, the nonlinear effects take over and we have a catastrophic blowup, as we argued above.

Next, we show results of the conformally rescaled system of Sec. IV, using $\xi=1$, and two different values of σ : σ

$=0$ (no use of the Hamiltonian constraint) and $\sigma=1$ (use of the Hamiltonian constraint to completely eliminate the Ricci scalar from the evolution equation for \tilde{A}_{ij}). From our analysis we expect the system with $\sigma=0$ to have an exponentially growing mode and thus to be very unstable. The $\sigma=1$ should only have the zero speed modes and should be much more stable (but still not completely stable). Figure 5 shows the rms of the Hamiltonian constraint for these two runs. We see that our predictions are indeed correct, the $\sigma=0$ run becomes rapidly unstable and crashes at $t=4$, while the $\sigma=1$ is far more stable and only crashes at $t=33$.

We now show the results of the choice $\sigma=0$, $m=1$, $\xi=0$ in Sec. V, as used by Baumgarte-Shapiro [29]. We have set $\text{tr}\tilde{A}_{ij}$ to zero at each step as discussed above. Figure 6 shows again a surface plot of g_{xx} along the x axis as a function of time (but notice the change of scale). The evolution now goes past $t=500$ with no trace of an instability. Figure 7 shows the rms of the Hamiltonian constraint for this run. The Hamiltonian constraint rapidly becomes much larger than in the ADM case at early times (by almost a factor of 10). However, it then stops growing and simply oscillates around a constant value, showing again no sign of the linear growth or the blowup that we saw for ADM.

Finally, we show results of a series of simulations done by keeping $\sigma=0$ and $\xi=0$, but changing the value of m (the amount of momentum constraint added to the evolution

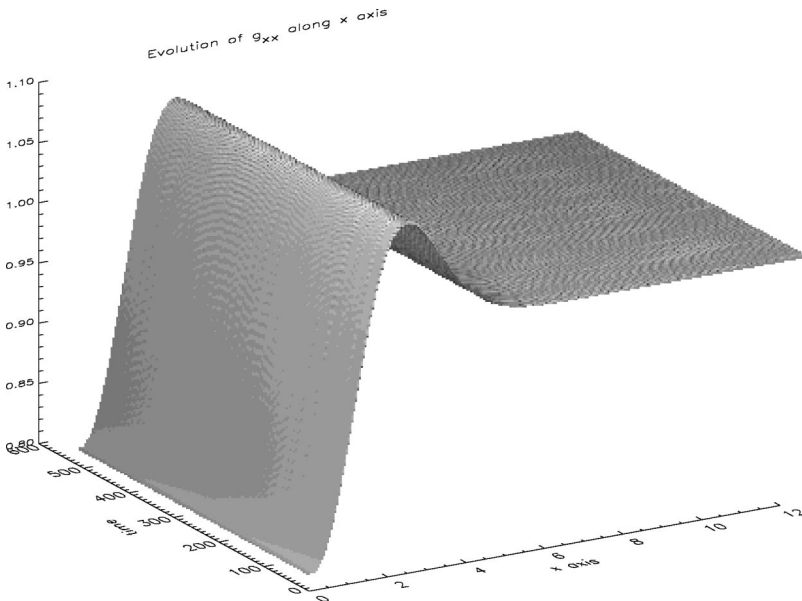


FIG. 6. Surface plot of g_{xx} along the x axis as a function of time for the simulation using the Baumgarte-Shapiro formulation.

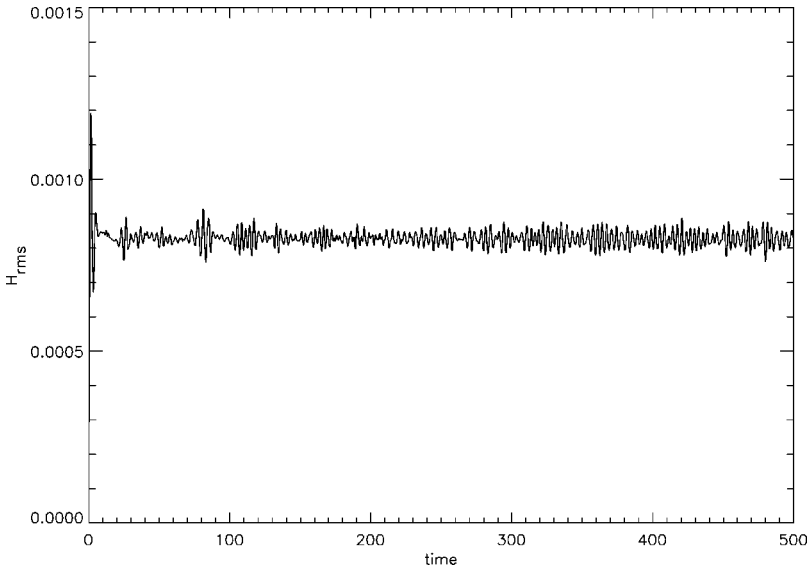


FIG. 7. Root mean square of the Hamiltonian constraint as a function of time for the simulation using the Baumgarte-Shapiro formulation.

equation of the $\tilde{\Gamma}$'s). Figure 8 shows the rms of the Hamiltonian constraint for runs with $m = \{0, 0.25, 0.5, 0.75\}$ (compare with the $m = 1$ case shown above). As expected from our analysis, we see that the cases with $m < 1/2$ rapidly become unstable. The simulation with $m = 0$ crashes at $t = 4$ while the one with $m = 0.25$ crashes at $t = 12$. On the other hand, the cases with $m \geq 0.5$ remain stable past $t = 400$.

VII. CONCLUSIONS

We have studied the stability properties of the standard ADM formulation of general relativity based on a linear perturbation analysis. We focus attention on the zero speed modes. We conjecture that the zero speed modes can cause instabilities in evolutions of the ADM system in its standard form. These instabilities do not have a numerical origin, but rather they correspond to genuine blowing-up solutions of

the differential equations.

We show that the zero speed modes come in two forms: a pure gauge mode that satisfies all the constraints, and is therefore a legitimate physical solution, and a series of non-physical constraint violating modes. We investigate the change in behavior of these modes going from the standard ADM formulation to the conformal-traceless (CT) systems of Shibata and Nakamura [28] and Baumgarte and Shapiro [29], and their derivatives. Two features we believe responsible for the better stability property of the conformal systems are identified. (1) The zero speed gauge mode is governed by an equation that is free from the complication of the Ricci tensor, thus decoupling it from the rest of the system. (2) The constraint violating zero speed modes, on the other hand, acquire a finite speed of propagation due to the introduction of extra first order degrees of freedom, and the use of the momentum constraints to modify the evolution equations

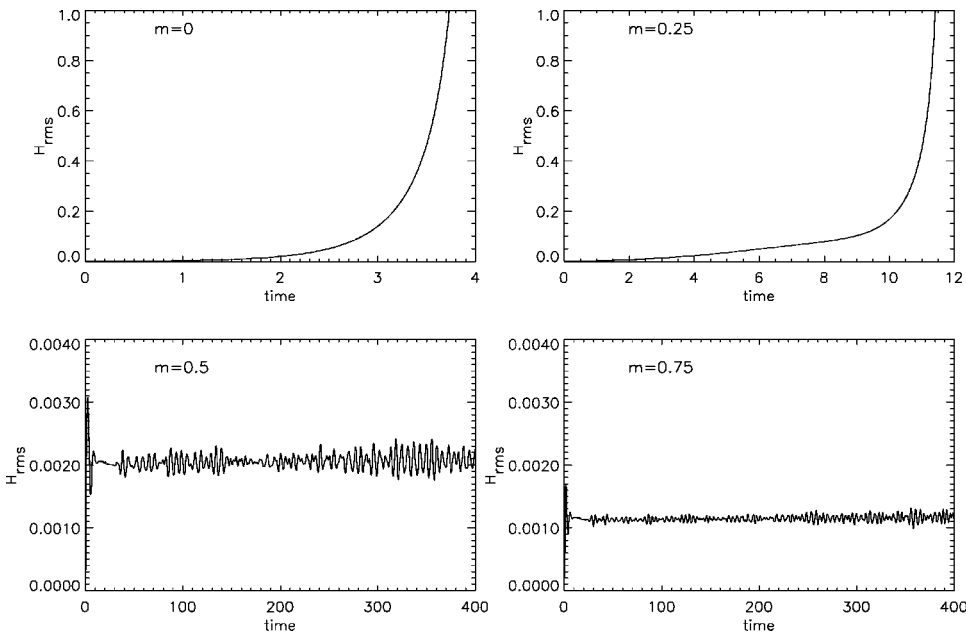


FIG. 8. Root mean square of the Hamiltonian constraint as a function of time for the simulation using the Baumgarte-Shapiro formulation with different multiples of the momentum constraint added to the evolution equation for the $\tilde{\Gamma}$'s (different values of the parameter m).

for these degrees of freedom. We present numerical examples to support our analysis.

We consider the study presented in this paper as a first step towards the understanding of the stability issue in the numerical evolution of the Einstein equations.

ACKNOWLEDGMENTS

The authors would like to thank A. Arbona, J. Baker, C. Bona, H. Friedrich, J. Massó, M. Miller, A. Rendall, and O. Reula for many helpful discussions. The research is supported in part by NSF Phy 96-00507, NASA NCCS5-153 and NRAC grant MCA 93S025.

APPENDIX A: FINITE DIFFERENCE APPROXIMATION TO THE LINEARIZED ADM EQUATIONS

We will consider a simple finite difference approximation to the linearized ADM evolution equations written in second order form. For this we start from Eqs. (6) and (7), and substitute one into the other to find

$$\partial_t^2 h_{ij} - \nabla_{\text{flat}}^2 h_{ij} = \partial_i \partial_j h - 2 \sum_m \partial_{(i} \partial_m h_{j)m}. \quad (\text{A1})$$

We now construct a simple second order finite difference approximation to this equation using standard centered differences,

$$\partial_t^2 f \approx \frac{1}{(\Delta t)^2} \delta_t^2 f_{\mathbf{m}}, \quad (\text{A2})$$

$$\partial_i^2 f \approx \frac{1}{(\Delta x)^2} \delta_i^2 f_{\mathbf{m}}, \quad (\text{A3})$$

with $f_{\mathbf{m}}^n = f(t = n\Delta t, x_i = m_i \Delta x)$ and

$$\delta_t^2 f_{\mathbf{m}}^n = f_{\mathbf{m}}^{n+1} - 2f_{\mathbf{m}}^n + f_{\mathbf{m}}^{n-1}, \quad (\text{A4})$$

$$\delta_i^2 f_{\mathbf{m}}^n = f_{m_i+1}^n - 2f_{m_i}^n + f_{m_i-1}^n. \quad (\text{A5})$$

Let us now consider a plane wave solution of the form

$$(h_{ij})_{\mathbf{m}}^n = \hat{h}_{ij} e^{i(n\omega\Delta t + \mathbf{m} \cdot \mathbf{k}\Delta x)}. \quad (\text{A6})$$

But notice now that we allow the waves to move along any direction. This is because even if different directions are equivalent from the analytic point of view, they are not equivalent numerically because the numerical grid introduces preferred directions.

If we substitute this into the finite difference approximation to Eq. (7) we find the following equation:

$$\frac{2}{\rho^2} [1 - \cos(\omega\Delta t)] \hat{\mathbf{h}} = \tilde{M} \hat{\mathbf{h}}, \quad (\text{A7})$$

where $\rho := \Delta t / \Delta x$ is the Courant parameter, $\hat{\mathbf{h}}$ is defined as before,

$$\hat{\mathbf{h}} := (\hat{h}_{xx}, \hat{h}_{yy}, \hat{h}_{zz}, \hat{h}_{xy}, \hat{h}_{xz}, \hat{h}_{yz}), \quad (\text{A8})$$

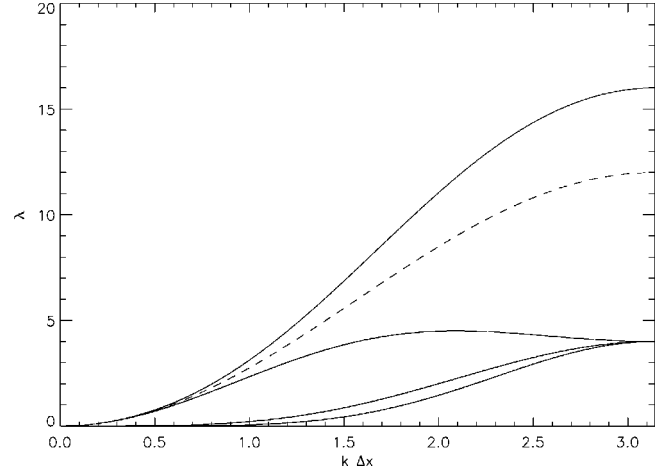


FIG. 9. Eigenvalues of the characteristic matrix \tilde{M} . The solid lines indicate the four distinct eigenvalues, while the dashed line indicates the eigenvalue one would obtain for the finite difference approximation to the simple 3D wave equation.

and \tilde{M} is the matrix

$$\tilde{M} = \begin{pmatrix} u_y^2 + u_z^2 & u_x^2 & u_x^2 & 2s_{xy} & 2s_{xz} & 0 \\ u_y^2 & u_x^2 + u_z^2 & u_y^2 & 2s_{xy} & 0 & 2s_{yz} \\ u_z^2 & u_z^2 & u_x^2 + u_y^2 & 0 & 2s_{xz} & 2s_{yz} \\ 0 & 0 & -s_{xy} & u_z^2 & s_{yz} & s_{xz} \\ 0 & -s_{xz} & 0 & s_{yz} & u_y^2 & s_{xy} \\ -s_{yz} & 0 & 0 & s_{xz} & s_{xy} & u_x^2 \end{pmatrix}, \quad (\text{A9})$$

where we have defined

$$u_i^2 := 2[1 - \cos(k_i \Delta x)], \quad (\text{A10})$$

$$s_{ij} := -\sin(k_i \Delta x) \sin(k_j \Delta x). \quad (\text{A11})$$

Let us now define

$$\lambda := \frac{2}{\rho^2} [1 - \cos(\omega\Delta t)]. \quad (\text{A12})$$

Equation (A7) now becomes

$$\tilde{M} \hat{\mathbf{h}} = \lambda \hat{\mathbf{h}}, \quad (\text{A13})$$

which is just an eigenvalue equation. Here we face one problem: the characteristic polynomial is of 6th order, and is difficult to solve exactly in the general case. We will then consider a couple of particular cases.

First, assume that the wave moves only on the x direction, so $k_y = k_z = 0$. In this case everything simplifies considerably, and we find that the eigenvalues of \tilde{M} are just $\lambda = 0$, with multiplicity 3 and $\lambda = u_x^2$, with multiplicity 3.

This has precisely the same structure we found before for the exact system of differential equations. The only differ-

ence being that the wave speed is now not quite 1. The wave speed in fact depends on the wave number k_x , and can be obtained from the dispersion relation

$$\frac{2}{\rho^2}[1 - \cos(\omega\Delta t)] = u_x^2. \quad (\text{A14})$$

Notice that for small $k_x\Delta x$ (large wavelengths compared to the grid spacing) this relation reduces to

$$\omega^2 = k_x^2, \quad (\text{A15})$$

which is what one expects. For smaller wavelengths we obtain wave speeds that are smaller than 1, showing the dispersive nature of the finite difference approximation.

The results above are not particularly surprising. One obtains essentially the same thing for the simple wave equation. The interesting case is when we consider waves moving in a direction different from the coordinate lines. We will then consider the particular case of waves moving in the diagonal direction, for which $k_x = k_y = k_z \equiv k$. The characteristic polynomial now does not simplify nearly as much, but one can still find the eigenvalues analytically. They are $\lambda = u^2 - s^2$, with multiplicity 2; $\lambda = u^2 + 2s^2$, with multiplicity 2, and $\lambda = \frac{1}{2}[5u^2 - 2s^2 \pm (9u^4 - 12s^4 + 12u^2s^2)^{1/2}]$, where

$$u^2 = 2[1 - \cos(k\Delta x)], \quad s^2 = \sin^2(k\Delta x). \quad (\text{A16})$$

The values of the different roots are shown in Fig. 9. The solid lines indicate the four distinct eigenvalues, while the dashed line indicates the eigenvalue one would obtain (also along the diagonal line) for the finite difference approximation to the simple 3D wave equation $\lambda = 3u^2$. The plot is only in the region $k\Delta x \in [0, \pi]$ since larger wave numbers can not be represented on the numerical grid ($k = \pi/\Delta x$ is the so-called ‘Nyquist’ frequency of our grid).

There are several things to notice from this result. First, we now have four distinct eigenvalues instead of two: the numerical grid has broken the degeneracy of the exact problem. Second, the three eigenvalues that were zero in the exact case are now only zero for $k=0$, and are clearly non-zero for any finite k . This shows that the zero speed modes have picked up a nonzero speed in the numerical approximation. This artificial speed is very small for large wavelengths (small k), but becomes considerable for smaller wavelengths. Finally, we see that for small values of k we recover the exact result: one eigenvalue vanishes as $k^6/12$, two as $k^4/4$, and the other three go to zero as $3k^2$, which is the correct result for waves traveling with a speed of 1 along the diagonal.

-
- [1] R. Arnowitt, S. Deser, and C. W. Misner, in *Gravitation: An Introduction to Current Research*, edited by L. Witten (Wiley, New York, 1962), pp. 227–265.
- [2] G. Allen, K. Camarda, and E. Seidel, gr-qc/9806036 (1998).
- [3] P. Anninos, J. Massó, E. Seidel, and W.-M. Suen, *Phys. World* **9**, 43 (1996).
- [4] B. Brügmann, *Int. J. Mod. Phys. D* **8**, 85 (1999).
- [5] G. B. Cook *et al.*, *Phys. Rev. Lett.* **80**, 2512 (1998).
- [6] H. Friedrich, *Proc. R. Soc. London* **A375**, 169 (1981).
- [7] H. Friedrich, *Proc. R. Soc. London* **A378**, 401 (1981).
- [8] Y. Choquet-Bruhat and T. Ruggeri, *Commun. Math. Phys.* **89**, 269 (1983).
- [9] H. Friedrich, *Commun. Math. Phys.* **100**, 525 (1985).
- [10] C. Bona and J. Massó, *Phys. Rev. Lett.* **68**, 1097 (1992).
- [11] C. Bona, J. Massó, E. Seidel, and J. Stela, *Phys. Rev. Lett.* **75**, 600 (1995).
- [12] Y. Choquet-Bruhat and J. York, *C. R. Acad. Sci. Paris* **321**, 1089 (1995).
- [13] S. Frittelli and O. Reula, *Phys. Rev. Lett.* **76**, 4667 (1996).
- [14] A. Abrahams and R. Price, *Phys. Rev. D* **53**, 1972 (1996).
- [15] H. Friedrich, *Class. Quantum Grav.* **13**, 1451 (1996).
- [16] M. H. van Putten and D. Eardley, *Phys. Rev. D* **53**, 3056 (1996).
- [17] A. Abrahams, A. Anderson, Y. Choquet-Bruhat, and J. York, *C. R. Acad. Sci. Paris* **323**, 835 (1996).
- [18] C. Bona, J. Massó, E. Seidel, and J. Stela, *Phys. Rev. D* **56**, 3405 (1997).
- [19] A. Abrahams, A. Anderson, Y. Choquet-Bruhat, and J. York, *Class. Quantum Grav.* **14**, A9 (1997).
- [20] A. Anderson, Y. Choquet-Bruhat, and J. York, *Topol. Methods Nonlinear Anal.* **10**, 353 (1997).
- [21] C. Bona, J. Massó, E. Seidel, and P. Walker, gr-qc/9804052 (1998).
- [22] A. Anderson and J. York, *Phys. Rev. Lett.* **82**, 4384 (1999).
- [23] M. Alcubierre, B. Brügmann, M. Miller, and W.-M. Suen, *Phys. Rev. D* **60**, 064017 (1999).
- [24] S. Detweiler, *Phys. Rev. D* **35**, 1095 (1987).
- [25] C. W. Lai *et al.*, report, Physics Department, Chinese University of Hong Kong, 1998.
- [26] O. Brodbeck, S. Frittelli, P. Hübner, and O. A. Reula, *J. Math. Phys.* **40**, 909 (1999).
- [27] J. Balakrishna *et al.*, *Class. Quantum Grav.* **13**, L135 (1996).
- [28] M. Shibata and T. Nakamura, *Phys. Rev. D* **52**, 5428 (1995).
- [29] T. W. Baumgarte and S. L. Shapiro, *Phys. Rev. D* **59**, 024007 (1999).
- [30] A. Arbona, C. Bona, J. Massó, and J. Stela, *Phys. Rev. D* **60**, 104014 (1999).
- [31] S. Frittelli and O. Reula, *J. Math. Phys.* **40**, 5143 (1999).
- [32] M. Alcubierre *et al.*, *Phys. Rev. D* **62**, 044034 (2000).
- [33] M. Alcubierre *et al.*, *Phys. Rev. D* **61**, 041501 (2000).
- [34] T. W. Baumgarte, S. A. Hughes, and S. L. Shapiro, *Phys. Rev. D* **60**, 087501 (1999).
- [35] R. Courant and D. Hilbert, *Methods of Mathematical Physics* (Wiley, New York, 1962).
- [36] B. Gustafsson, H.-O. Kreiss, and J. Oliger, *Time Dependent Problems and Difference Methods* (Wiley, New York, 1995).
- [37] P. Anninos *et al.*, *Phys. Rev. D* **56**, 842 (1997).
- [38] S. Frittelli, *Phys. Rev. D* **55**, 5992 (1997).